Chapter 2

Analytical techniques employed for characterization

This chapter is dedicated to introducing and illustrates the experimental techniques and methods used for present study. In this chapter the necessary basics and procedure of measurements will be briefly explained. In experimental condensed matter physics, acquiring a good quality sample is of paramount and prime need. It enables the further characterizations to be carried out confidently. That's why the sample preparation is one of the primary, crucial, important, careful and foremost steps. The next step is the collection of reliable experimental data. In the third and final step, suitable theoretical or explanatory physical models have to be employed to analyze the data based on which concrete arguments can be put forward to explain the physical properties.

2.1 Introduction

This chapter outlines the thin film fabrication and characterization techniques used in the present study leading to the thesis. These include the techniques for the synthesis and characterization of semiconducting alloys in the form of bulk and thin films. In the section 2.2.2.1 details of the experimental setup and the procedure involved in the thermal evaporation technique will be discussed. In order to characterize the thin films, different techniques have been employed. The techniques involve X-ray diffraction for structural analysis; Atomic Force Microscopy is used for surface topography and surface roughness determination. Scanning Electron Microscopy is used to get information about the sample including external morphology (texture), chemical composition, crystalline structure and orientation of materials making up the sample. Energy Dispersive X-ray Analysis (EDXA) technique is used for elemental analysis. Four probe resistivity measurement is used to observe the temperature dependent resistance of $Fe_{0.008}Sb_{1-x}Se_x$ thin film, two probe resistivity setup is used to observe the resistance as a function of temperature in $Fe_{0.01}Ge_{1-x}Sb_x$ thin films and Quantum design Physical property measurement system (QD-PPMS) is used to investigate the different electrical properties of transition metal doped InSb thin films. Magnetic force microscopy (MFM) is used to evaluate the magnetic interaction at the surface of thin films. Mossbauer Spectroscopy is used to see the hyperfine interaction in Iron doped InSb bulk systems. In the following sections, the synthesis and characterization techniques involved in the present work will be discussed.

2.2 Sample preparation methods

2.2.1 Bulk sample preparation

The materials which maintain their required properties even under extreme

environmental condition are the top priority among researchers. In general the present work is aimed to find ways of increasing quality and productivity, while reducing the manufacturing cost. This could be achieved by the development of better processing techniques. Quality of materials used to prepare alloys and compounds have a very important role in properties of thin films. To prepare the thin films, bulk alloys need to be prepared.

To prepare bulk alloys, elements of purity better than 99.999 % (Alfa Aeser USA) are taken for making the bulk alloys. The bulk alloys of $Fe_{0.01}Ge_{1-x}Sb_x$ (chapter 3), $Fe_{0.008}Sb_{1-x}Se_x$ (chapter 4) are prepared by Argon arc furnace, while the Transition metal doped InSb bulk system (chapter 5) is prepared using vacuum quartz tube sealing method. After the preparation of these bulk alloys, thin film is grown on Silicon substrate using thermal evaporation technique.

2.2.1.1 Argon arc melting method

To prepare the $Fe_{0.01}Ge_{1-x}Sb_x$ and $Fe_{0.008}Sb_{1-x}Se_x$ bulk alloy system, argon arc furnace is used. These appropriate amount of samples are loaded on copper hearth and melted several times in the presence of 400 Torr Argon atmosphere. Argon gas is used to make the chamber free from other gas. For this, chamber is purged and sealed using argon gas at least three times. Tungsten tip is used for producing arc. Single Arc furnace from M/s Centorr Inc., USA is used for this purpose. The operating current to produce an arc is in the range 20-60 A. The used current to generate arc is 50 A in this case. A Titanium ball is used as Getter element. At first, this Titanium ball is melted for a few seconds so that it can absorb all reactive gases like Oxygen which is present in the furnace. Then the ingredients are melted several times for better homogeneity and mixing to get ball shape. Arc furnace consists of separate water cooled top and bottom sections made of brass separated by transparent quartz cylinder tubing.

The top or negative section contains swivel ball assembly with an electrode for striking an arc. The bottom or positive section includes a tapered opening for access of the hearth. Each section is individually fixed to wooden base support and electrically insulated by quartz tube. The hearth is mounted on the furnace by inserting it into tapering cavity, supported by the pair of toggle clamp. The copper electrode has throated tungsten tip, is mounted into swivel ball that allows vertical as well as angular movement. Ports are provided for Argon gas inlet, evacuation kit and vacuum gauge.

Figure 2.1: Photograph of Argon arc furnace system (UGC DAE CSR, Indore (M.P.), India)

The top and bottom sections are water cooled by a chiller and water pump assembly. The evacuation kit comprises of a rotary pump. Partial pressure of Argon gas is required to strike an arc. The water cooled Cu electrode can withstand high currents. A foot operate current switch is provided for amperage control. It operates at maximum of 300 Amps, 32-volt DC. The Argon arc furnace facility is used at UGC DAE CSR lab Indore (M. P.), India. The photograph of Argon arc furnace is shown in **figure 2.1**.

2.2.1.2 Vacuum sealing in quartz tube

To prepare the transition metal doped InSb bulk alloy system, required amount

of the materials is taken in small quartz ampoules, which is then evacuated to $>10^{-5}$ Torr and sealed. The ampoules are heated in an oxy-butane flame. The melted samples are allowed to cool to room temperature and again re-melted. The process is repeated a number of times to ensure homogeneity before they are finally quenched in water.

2.2.2 Thin Film Fabrication Technique

Thin film of magnetic materials and semiconductor materials have found wide commercial application for data storage and data processing in computers and control systems.

The thin film growth technique plays a significant role in governing the properties of thin films, because the material deposited by two or more than two different techniques usually has different physical properties. This is due to the fact that the electrical and physical properties of these films strongly depend on the structural, morphology and the nature of the impurity present. Moreover, the film grown by particular technique may often have different properties due to the involvement of various deposition parameters. The properties however, can be tailored by controlling the deposition parameters. It is, therefore, essential to make a detailed investigation of the relationship between the properties of these films and the method of deposition.

The basic steps involved in the thin film deposition are: taking the material in appropriate quantity, transport and deposition of material. The techniques employed for the preparation of the thin films are physical vapor deposition (PVD), chemical vapor deposition (CVD) and electrochemical deposition (ECD). The PVD technique depends on the evaporation or ejection of material from source, whereas chemical methods depend on a specific chemical reaction [1-3]. The physical methods include PVD, molecular beam epitaxy, Ion beam sputtering, flash evaporation technique and ion plating. The objective of these deposition process is to transfer atoms from a source to

substrate where film formation and growth proceeds. By evaporation, atoms are removed from the source by the thermal heating process, whereas in sputtering, they are dislodged from target surface through the impact of gaseous ions. The molecular beam epitaxy produces epitaxial films by condensation of atoms from Knudsen source under ultrahigh vacuum. If the evaporated material is transported through a reactive gas, the deposition technique is called reactive evaporation; Flash evaporation technique is used when we have to deposit a multicomponent material that cannot be heated to the evaporation point together. Ion plating refers to a process in which the substrate and film are exposed to a flux of high energy ions during deposition. The chemical vapor deposition is the process of chemically reacting a volatile compound of a material to be deposited, with other gases or condensation of a compound from the gas phase onto substrate. Here reaction occurs to produce a solid deposit. The various chemical methods include gas-phase deposition methods and solution techniques. The gas-phase methods are chemical vapor deposition (CVD) [4-5] and atomic layer epitaxy (ALE) [6] while spray pyrolysis [7], sol-gel [8], spin-[9] and dip-coating [10] methods employ the precursor solution. Each of the above methods has its own advantages and disadvantages and we will restrict our discussion to those methods are used in the present study. The vacuum thermal evaporation technique for the preparation of thin film in the present investigations and are discussed in detail below.
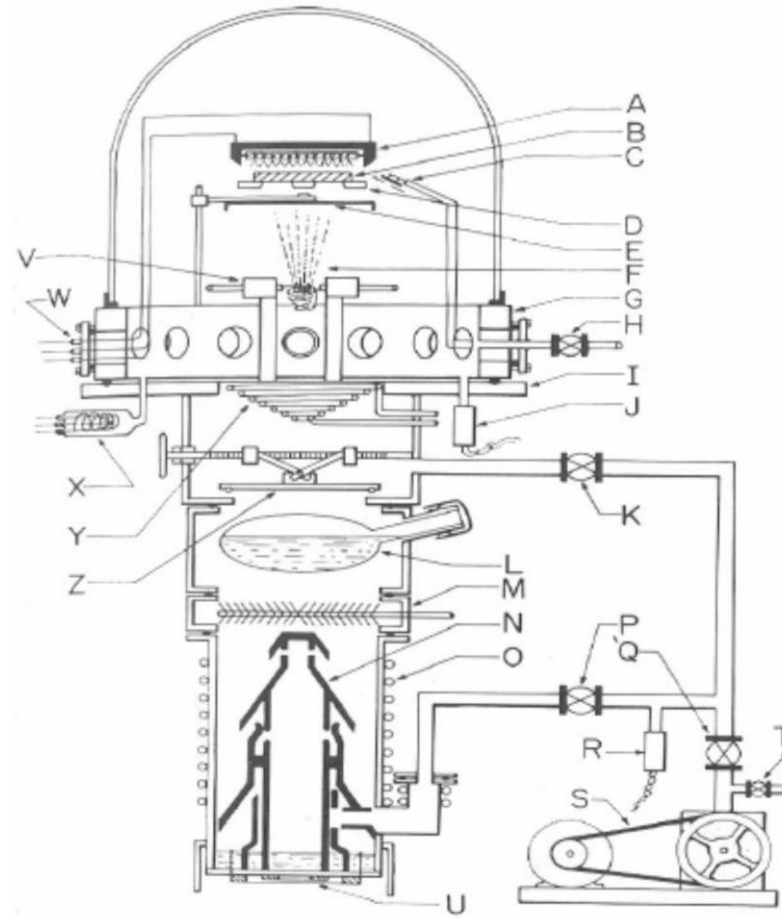
2.2.2.1 Thermal Evaporation Technique

A large number of semiconductor and metallic materials can be evaporated in vacuum using thermal evaporation technique such as ZnO [11], CdS [12], SnO_2 [13], Sb_2O_3 [14], ZnS [15], SnSe [16]. All these thin films grown using this method have a good uniformity. This technique is one of the most commonly used techniques for metal and semiconductor samples [11-19]. To grow the $Fe_{0.01}Ge_{1-x}Sb_x$, $Fe_{0.008}Sb_{1-x}Se_x$,

different transition metal doped InSb and Sb-Se bilayer thin films, vacuum thermal evaporation technique is used. A solid material is evaporated by heating it to a sufficiently high temperature and re-condensed onto a substance to form a thin film. The heating (Joule heating effect) is carried out by passing a large current through a filament container which has a finite electrical resistance. Once the metal is evaporated, its vapor undergoes collisions with the surrounding gas molecules inside the evaporation chamber. As a result, a fraction of particles are scattered within a given distance during their transfer through the ambient gas. The pressure, lower than 1×10^{-5} Torr is used for deposition process. The substrate to source distance is of approximately 20 nm in a vacuum chamber.

Schematic representation of the vacuum unit ('HINDHIVAC' vacuum coating unit) along with all the components is shown in the **figure 2.2** essentially, it includes a bell jar made up of metal, with two quartz view posts, connected to a rotary pump, a diffusion pump (DP), a roughing valve (connecting the rotary pump to the chamber), a backing valve (connecting the rotary pump to the diffusion pump) and a high vacuum valve (baffle, which connects the diffusion pump to chamber).

In the present study, for making of bulk samples, the following highly pure elements are taken:

1. Fe, Ge and Sb for $Fe_{0.01}Ge_{1-x}Sb_x$ system (detailed in chapter 3).

2. Fe, Sb and Se for $Fe_{0.008}Sb_{1-x}Se_x$ system (detailed in chapter 4).

3. Transition metals (Fe, Co, Mn and Ni), In and Sb, for TM doped InSb system (detailed in chapter 5).

Figure 2.2: Schematic diagram and different parts of thermal evaporation technique

These materials are purchased from Alfa Aeser USA (5N purity) and grinded thoroughly in an agate mortar, to form a fairly homogeneous physical mixture of elements to make desired compositions of Sb and Se to form $Fe_{0.01}Ge_{1-x}Sb_x$ and $Fe_{0.008}Sb_{1-x}Se_x$ bulk and thin films respectively. To make TM doped InSb thin films highly pure (5N purity) transition metals of Fe, Co, Ni and Mn is used. The prepared mixture of these alloys is kept in a Molybdenum boat and thermally evaporated on to the Silicon substrate by keeping at an ambient temperature.

The schematic diagram of thermal evaporation technique is shown in **figure 2.2**.

Different parts of thermal evaporation unit are as below.

    A- Quartz iodine lamp heater

    B- Substrate

C- Quartz crystal rate controller and deposition monitor

D- Substrate mask

E- Shutter (Mechanical or Electromagnetic)

F- Vapors from evaporation source

G- Adapter collar between the bell jar and the pump baseplate flange

H- Air-inlet valve

I- Baseplate flange

J- Pirani or thermocouple gauge

K- Roughing valve

L- Liquid-air trap

M- Cooled chevron baffles

N- Diffusion pump

O- Cooling coils

P & Q- backing valves

R- Pirani gauge

S- Fore pump with air-inlet valve T

U- diffusion-pump heater

V- Filament holders

W- Multiple feed through

X- Ionization gauge

Y- Meisner trap

Z- Baffle valve.

Thin films properties are very sensitive to their thickness so film thickness is controlled by Tolansky's Fizeau Fringe Method.
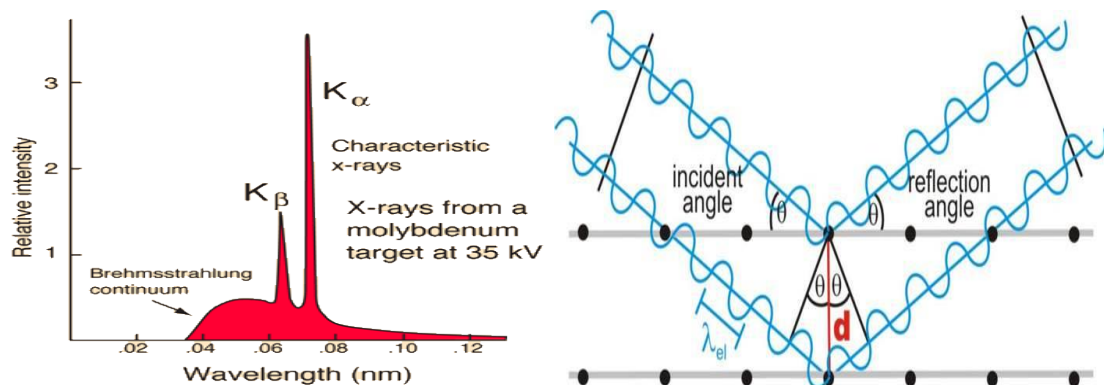
2.3 Structural studies

For the structural studies of bulk and thin films X-ray diffraction is used.

2.3.1 X-Ray Diffraction (XRD)

X-rays are produced by bombarding a metal target of Copper (or Molybdenum) with an accelerating electrons emitted by the hot filament (often tungsten) by the application of voltage. The incident electrons have sufficient energy to ionize electrons from the K-shell (1s) of the target atom. The vacancy state of K shell is filled by the transition of less energetic electron of L-shell, resulting into K-alpha radiations (K_α) called X-rays.

Characteristic x-rays are emitted when electrons make transitions between the lower atomic energy levels. Bremsstrahlung or Braking or continuous X-ray is emitted when electrons are decelerated on bombarding at metal target.

Figure 2.3: *Characteristic and bremsstrahlung X-ray's (in left) and constructed interference waves of reflected waves (in right)*

X-ray diffraction is a powerful technique for structural characterization based on Bragg's law.

Bragg's law: $n\lambda = 2dsin\theta$, where n is the order of diffraction, θ is the Bragg angle, d is interplaner distance and λ is wavelength of the X- ray source.

Bragg's law conditions are {1} angle of incident = angle of scattering (Elastic scattering), {2} Reflected rays should interfere to get constructive interference. {3} the path length difference is equal to the integer number of wavelength. Characteristics of X-rays and constructive interference reflection of X- rays are shown in **figure 2.3**.

XRD measurements are performed using CuK$_\alpha$ (wavelength = 1.5405 Å) radiation on a powder specimen with a Bruker D8 advance X-ray diffractometer. The data collected in 2θ scan with angular speed of 2 degree per minute and a step size of 0.02 degree.

Crystallite size determination

Scherrer [20] first showed that the mean dimension D of the crystallite is related to the X-ray diffraction broadening β by the equation.
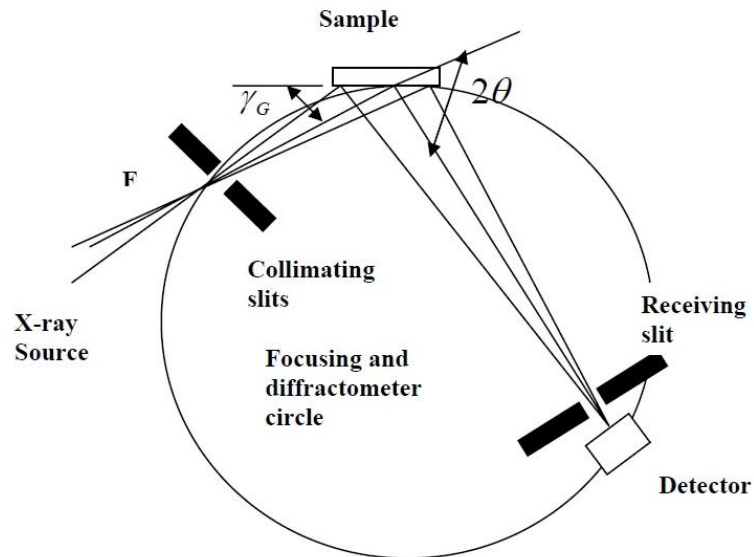
$$D = \frac{K\lambda}{\beta Cos\theta}$$

Where K is constant and approximately the value is 1 and related to crystallite shape, β is Full Width at Half Maxima (FWHM) of the diffraction peak.

The structural studies of thin films are characterized by grazing angle X-ray diffraction (GAXRD) technique using Bruker D8 Advance X-ray diffractometer. The X- rays are produced using a sealed tube using CuK$_\alpha$, (λ = 1.5405 Å) radiation. The X-rays are detected using a fast counting detector based on silicon strip technology (Bruker LynxEye detector). This configuration allows the use of a GAXRD. The GAXRD pattern is monitored at RT with a constant rate of 0.05°/3s at grazing angle 0.5°. The GAXRD is discussed below.

2.3.1.1 Grazing Angle X-ray diffraction (GAXRD)

It is sometimes very difficult to analyze thin films due to their small diffracting volumes, which results in low diffracted intensities compared to the substrate and background. This combination of low diffracted signal and high background make it

very difficult to identify the presence of phases. So, special techniques must be employed when analyzing thin films. The most common technique for analyzing thin films as thin as 100 Å is to use a grazing incidence angle arrangement. The glancing angle diffraction technique is used when the information needed lies in the thin top layer of the material **[21]**. **Figure 2.4** shows Seemann-Bohlin parafocusing geometry which is commonly used in the study of thin films. For the Seemann- Bohlin geometry (**figure 2.4**) the incident X-rays impinge on a fixed specimen at a small angle, γ_G (typically $10°$ to $30°$) and the diffracted X-rays are recorded by a detector that moves along the focusing circle.

Figure 2.4: Seemann-Bohlin diffractometer. The point F is either the focal point on an X-ray tube or the focal point of a focusing monochromator

This method provides good sensitivity for thin films, due to parafocusing and the large diffracting volume, which results from γ_G being small and the X-ray path length in the film being large (proportional to $1/\sin \gamma_G$). By increasing the path length of the incident X-ray beam through the film, the intensity from the film can be increased, while at the same time, the diffracted intensity of the substrate can be reduced. Overall, there is a dramatic increase in the film signal to the background

ratio. On applying grazing angle the path length increases resulting into increase in diffraction volume. This is the reason for the increased signal strength. During the collection of the diffraction spectrum, only the detector rotates through the angular range, thus keeping the incident angle, the beam path length and the irradiated area constant.
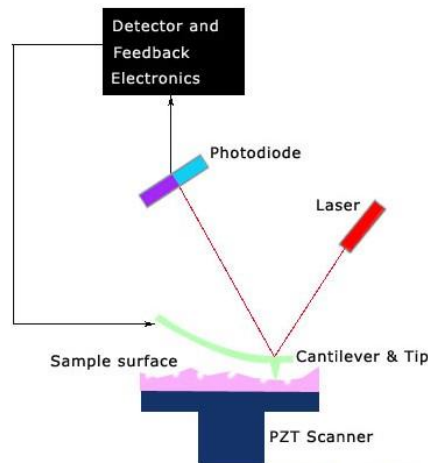
The GAXRD is used for structural study of $Fe_{0.01}Ge_{1-x}Sb_x$ (chapter 3), $Fe_{0.008}Sb_{1-x}Se_x$ (chapter 4) and Transition metal doped InSb (chapter 5) thin films respectively.

2.4 Surface study

Surface studies of the thin films are done using Atomic Force Microscopy and Scanning Electron Microscopy.
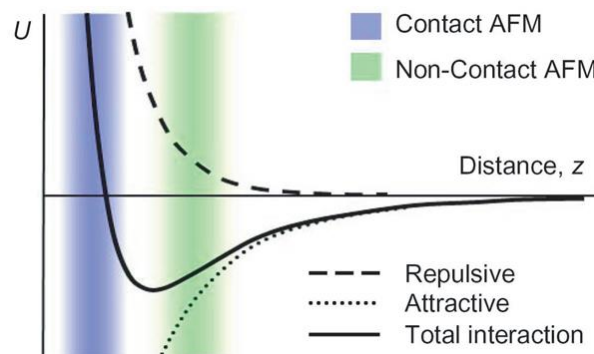
2.4.1 Atomic Force Microscope (AFM)

During the past decade, the atomic force microscopy has been developed from an exotic instrument into a relatively widespread surface imaging and probing instrument. Atomic force microscopy (AFM) and its related techniques have proliferated successfully in many fields. Today this method is used to obtain the high-resolution static and dynamic images in the investigation of the physical and mechanical properties of the thin films of different materials as well as biological molecules. In the present work AFM is used to study the surfaces of the transition metal doped alloys and compound thin films. The schematic diagram of the instrument is shown in **figure 2.5**.

Figure 2.5: Schematic instrumentation diagram of a basic AFM

The AFM uses the interatomic forces that exist between atoms and molecules. During the operation, tip mounted on a cantilever is brought very close to the sample, so that the atoms of the tip interact with the atoms of the sample. This interactive force affects the cantilever and this causes changes in either the static deflection or its dynamic properties. These are precisely measured to extract the image of the samples. There are two regimes of force that the tip experiences while scanning close to the sample surface shown in **figure 2.6**.

Figure 2.6: Nature of forces in the Contact and Non-contact mode of AFM operation

One of them is the short-range and other long- range forces specific to the tip sample system. Short-range forces comprise of the chemical forces with a range less than a nanometer. These forces are mildly attractive, but immensely repulsive at small separations. The long-range forces include the Van der Waals, magnetic and electrostatic forces with an interaction range up to 100 nm. The Van der Waal forces

are ubiquitous and are always attractive making the typical long-range forces attractive. In ambient conditions capillary and adhesion forces come into play due to the adsorption of water and other molecules on the sample surface. The short-range forces are a consequence of the overlap of electron clouds and ionic repulsion. The variation of these forces on the atomic scale leads to atomic resolution in AFM. For very small separations, the short-range forces will be dominant and the sample atoms closest to the tip resulting in atomic resolution, contribute to almost all the information. At large separations, the long-range forces dominate and the resolution deteriorates due to the many-atom interaction between the tip and the sample. AFM has ability to create three-dimensional micrograph of sample surface with a resolution down to the Nano and Angstrom scale. It is also capable of measuring the local property - such as height, optical absorption, conductivity or magnetism with a probe or 'tip' placed very close to the sample. The small probe-sample separation makes it possible to take measurement over a small area. The Van der Waal's interaction governs AFM. In AFM, a sensor is a cantilever with an effective spring constant k. At the end of the lever, there is a sharp tip (Silicon nitride), which is used to sense the force between the tip and the sample. Lever deflects in accordance with the force acting on tip. Detector measures the deflection of the lever. In AFM, the laser feedback detection system is used, which can determine the force on the tip by using Hooks law, $F = k.z$, where z is the cantilever displacement. If the sample is scanned under the tip, the force between tip and sample surface gives the image of the sample surface. By scanning the movement of AFM cantilever over a sample surface and recording the deflection of the cantilever the local height of the sample is measured. For the present surface study, Nanoscope-III Digital instrument from USA in contact mode at UGC DAE CSR Indore has been used.

The Atomic force microscopy technique is used for the surface studies of $Fe_{0.01}Ge_{1-x}Sb_x$ (chapter 3), $Fe_{0.008}Sb_{1-x}Se_x$ (chapter 4) and Transition metal doped InSb (chapter 5) thin films.
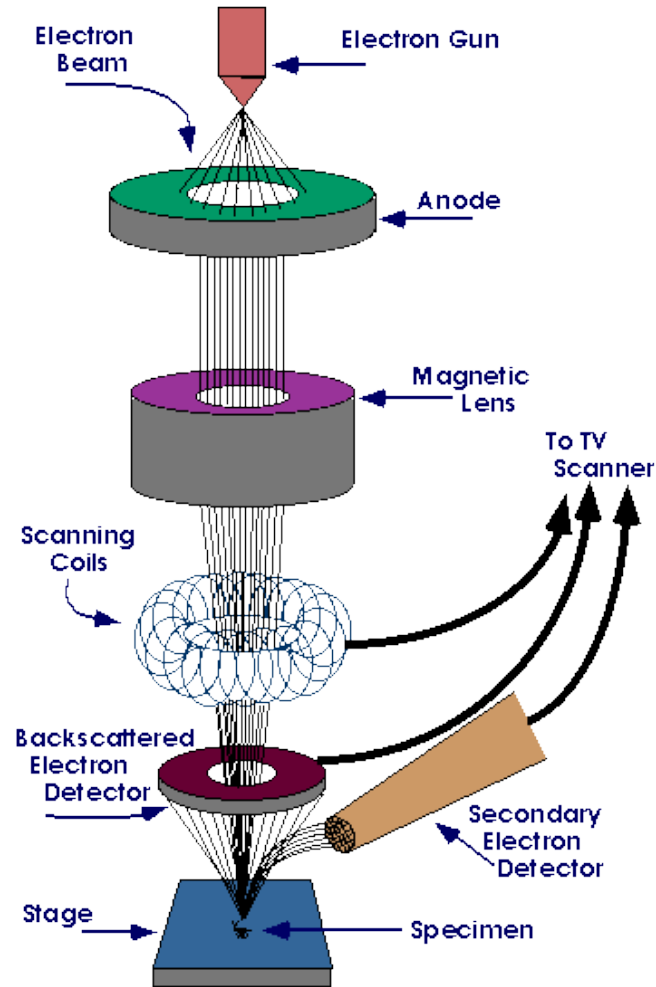
2.4.2 Scanning Electron Microscope (SEM) and Energy Dispersive X-rays Analysis (EDXA)

An electron microscope is employed to magnify things on a fine scale. Electron microscope uses a beam of electrons to illuminate a specimen and create a highly-magnified image. Electron microscope has much greater resolving power and greater magnification than light microscopes because the de Broglie wavelength of an electron is much smaller than that of a photon of visible light. Both electron and light microscopes have limited resolution. The electron microscope uses electrostatic and electromagnetic lenses in forming the image by controlling the electron beam to focus it at on a specific plane relative to the specimen. This is analogous to a light microscope using glass lenses to focus light on or through a specimen to form an image.

In SEM, a source of electrons is focused in vacuum into a fine probe, i.e. rastered over the surface of the specimen. The electron beam passes through scan coils and objective lens that deflect the beam horizontally and vertically so that the beam scans the surface of the specimen (**figure 2.7**).

As the electron beam penetrates in the surface of specimen, a number of interactions occur that can result in the emission of electrons or photons from or through the surface. So the fraction of the emitted electrons can be collected by appropriate detectors and the output can be used to modulate the brightness of a Cathode Ray Tube (CRT) whose x- and y- inputs are driven in synchronism with the x-y voltages rastering the electron beam.

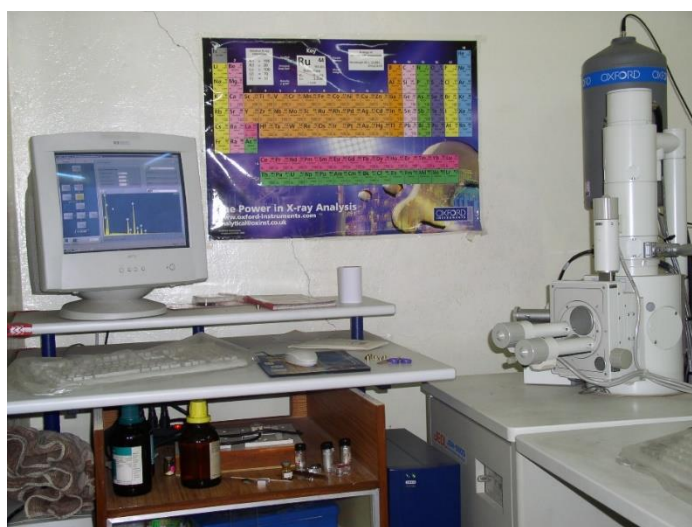**Figure 2.7:** *Schematic view of a Scanning Electron Microscopy (SEM)*

In this way an image is produced on the CRT. Every point that the beam strikes on the sample is mapped directly onto a corresponding point on the screen **[21]**. As a result, the magnification system is simple and linear magnification is calculated by the equation

$$M = L/I$$

Where L is the raster's length of the CRT monitor and l the raster's length on the surface of the sample. SEM works with a voltage between 2 to 50 KV and its beam diameter that scans the specimen is 5 nm − 2 μm.

The principle images produced in SEM are of three types: secondary electron images, backscattered electron images and elemental X-ray maps. Secondary and backscattered

electrons are conventionally separated according to their energies. When the energy of the emitted electron is less than about 50 eV, it is referred to as a secondary electron and backscattered electrons are considered to be the electrons that exit the specimen with energy greater than 50 eV [22]. Detectors of each type of electrons are placed in the microscope in proper positions to collect them. The morphology of synthesized material is monitored by a JEOL make Scanning Electron Microscope, model number JSM 6380 LV (**figure 2.8**).

Figure 2.8: Photograph of the laboratory SEM and EDXA

The accelerating voltage is fixed at 20 KV and filament current is kept nearly 85 μA to 100 μA to conduct morphological analysis. Inside the SEM chamber, the vacuum is created less than 10^{-7} Torr for minimizing the impurities and viewing the sharp surfaces of the sample. The magnifications of the images are varied as per the image clarity. All micrographs are viewed into two electron image mode (a) Secondary Electron Image (SEI), and (b) Backscattered Electron Image (BEI). Compositional analysis of the material may also be obtained by monitoring the energy dispersive analysis of secondary X-rays (EDXA). The SEM and EDXA measurements are used for the surface and elemental study of SbSe bi-layer thin films system grown on quartz substrate.

2.5 Electrical Studies

The electrical studies of the thin films are done using four probe, two probe, physical property measurement system (PPMS). These techniques are discussed below respectively.

2.5.1 DC resistivity

The fundamental electrical characterization of a semiconducting thin film is studied by DC resistivity. There are many methods to determine the resistivity of a thin film. Some important methods are two probe, four probe [25] and Van der Pauw method [23-25]. The dc resistivity of a thin film is easily measured by applying full width contacts at each end of a rectangular sample and directly measuring the resistance using an ohmmeter. The resistivity is given by

$$\rho = \frac{R \times T \times W}{l}$$

Where R is measured resistance, T is the thickness of the thin film, W is the width of film and l is the distance between two metallic (as Indium) contacts. This measurement provides accurate assessment of resistivity only if the contact resistance is negligible as compared to specimen resistance. The contacts can be easily evaluated by preparing two identical samples with different length to width ratios, if the measured resistance is proportional to the length to width ratio; the contact resistance is indeed negligible.
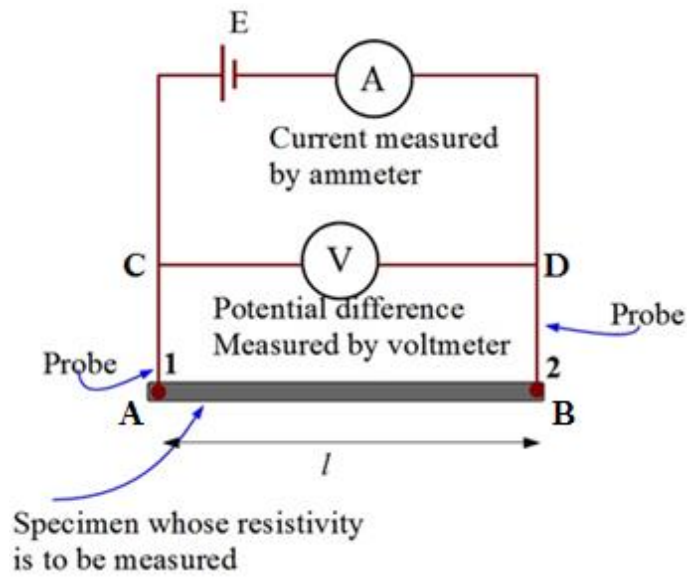
2.5.1.1 Two Probe Method

For two probe method condition is

$$V = V_{AC} + V_{AB} + V_{BD}$$

$$V = IR_L + IR_S + IR_L \dots\dots\dots\dots\dots\dots\dots\dots(2.6)$$

Where, R_L is the load resistance and R_S is resistance of the sample.

For the case of $R_S < 2R_L$ the determination of R_S by two probe technique has no significance. But it can be used in the case $R_S \gg 2R_L$ with an error R_L/R_S considering that the internal resistance of the voltmeter is finitely large. Thus, for the study of electrical properties of semiconducting thin films which have resistance of the order of $M\Omega$ (*i. e.* in case of $Fe_{0.01}Ge_{1-x}Sb_x$ thin films) two probe method is used. The circuit diagram of the two probe set up is shown in the **figure 2.9**.
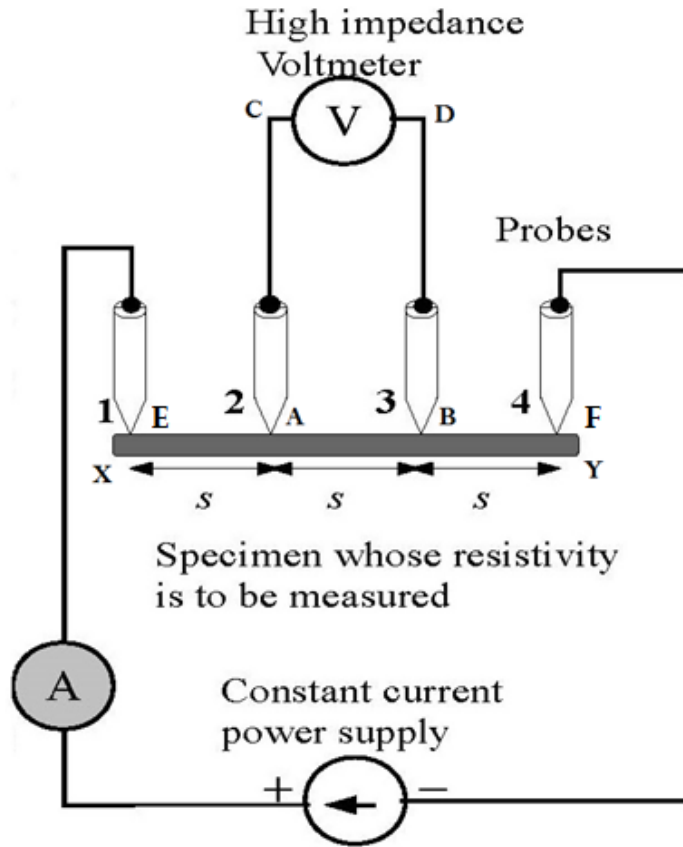

Figure 2.9: Schematic diagram of two probe Resistivity Measurement

Two probe method cannot be used for materials having random shapes.

In the present study the two probe method is used for the electrical studies of the Fe doped $Ge_{1-x}Sb_x$ alloy thin films $Fe_{0.01}Ge_{1-x}Sb_x$. The $Fe_{0.01}Ge_{1-x}Sb_x$ thin films thermally evaporated on Silicon substrate have the resistance of the order of Mega-Ohms at RT.

2.5.1.2 Four probe Method

The four-point probe method consists of equidistant metal tips with finite radius. A high impedance current source is used to supply current through the outer two probes (E and F) as shown in **figure 2.10**. A voltmeter measures the voltage across the inner two probes (A and B) to determine the specimen resistivity.

Figure 2.10: Schematic diagram of four probe Resistivity Measurement

The inner probes draw no current because of the high input impedance voltmeter in the circuit. The unwanted voltage drops at inner points (A and B) points caused by contact resistance between probes and the sample is eliminated from the potential measurements. Since these contact resistances are very sensitive to surface condition. The electric current carried through the two outer probes, sets up an electric field in the sample. The two inner probes measure the potential difference point A and B.

However, when one is measuring a small sample resistance, especially under variable temperature conditions, the contact resistances can dominate and completely obscure changes in the resistance of the sample itself. In the case of $R_S < 2R_L$, one has to use the four probe technique to eliminate the error induced in the measurement by the load resistance. In case of four probe method

$$V = V_{AC} + V_{AB} + V_{BD} \qquad (2.7)$$

39

Since no current pass through the loop ABCD, as internal resistance of voltmeter is infinitely large we have

$$V_{AC} \approx 0 \text{ and } V_{BD} \approx 0$$
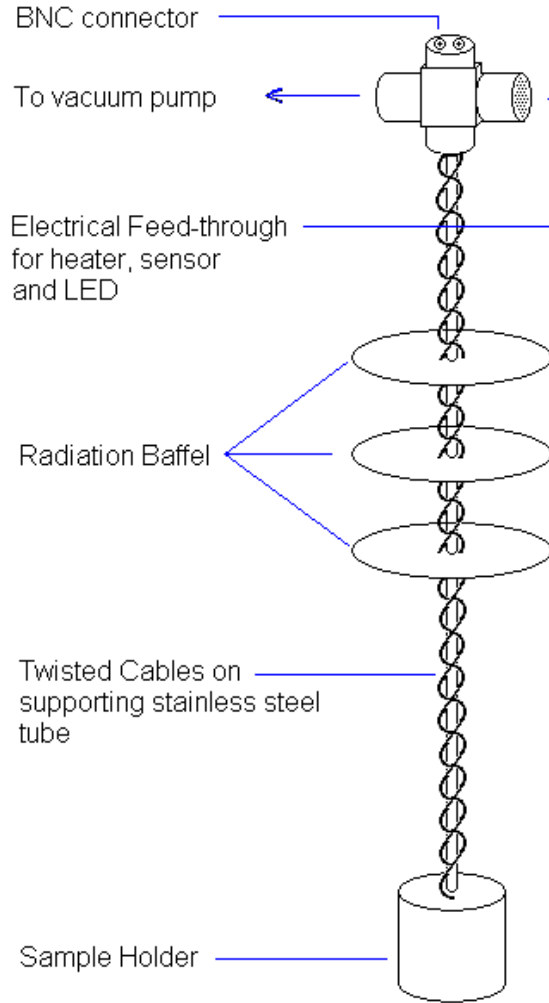
$$\text{Then, } V = V_{AB}$$

Thus one can measure low resistance up to a good accuracy except for the error due to leakage current through voltmeter.

The thermal activation energy can be calculated by using Arrhenius equation.

$$\rho = \rho_0 \, exp\left(\frac{E_a}{K_b T}\right)$$

Where ρ_0 is a constant, E_a is the activation energy gap, K_b is the Boltzmann constant and T is absolute temperature. The slope of the $\ln\rho$ versus (1/T) leads to the estimation of the activation energy.

In the present setup Kiethley electrometer is used to measure the resistance of the sample. In the present work, the resistivity measurement from low temperature to 400 K is done. A 617 programmable electrometer, Lakeshore temperature controller along with Platinum Resistance Thermocouple (PRT) sensor is used. These are connected to measure the temperature of the sample. The heater coil is made up of manganese wire. The dip stick holder is shown in **figure 2.11**. The whole setup is placed in cryostat and vacuum (10^{-5} mbar) is provided by the diffusion rotatory assembly. The sample is glued with GE varnish on the sample holder. The sample contacts are made up of copper wire by using Indium metal. The insert thus developed is used in conjunction with the cryostat having liquid nitrogen as coolant **[26]**.
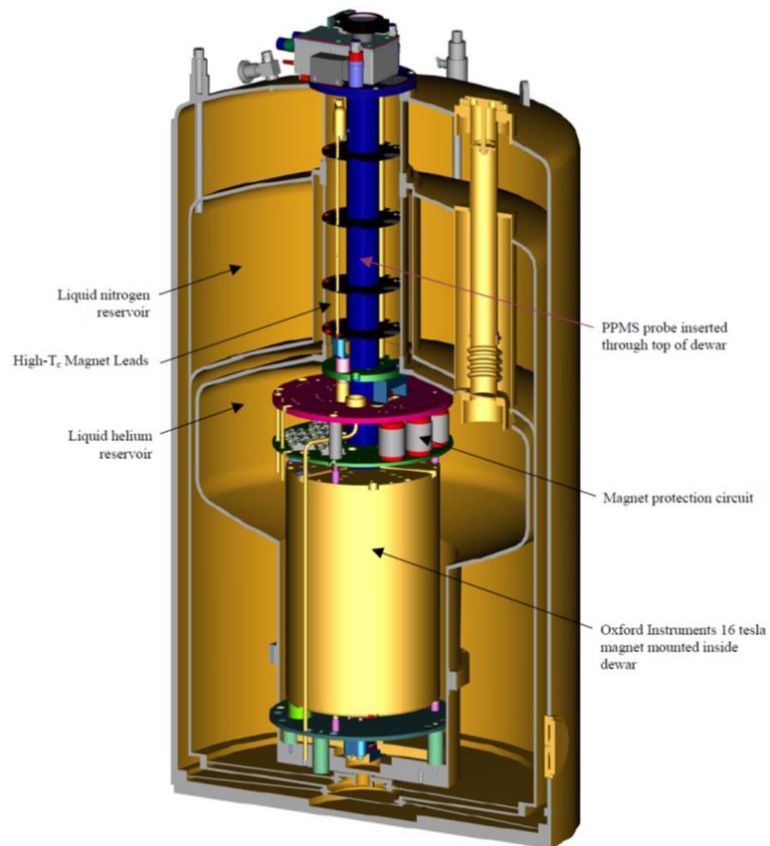
The four probe method is used for the electrical studies of the very dilute Fe doped $Sb_{1-x}Se_x$ alloy thin films *i. e.* $Fe_{0.008}Sb_{1-x}Se_x$. The $Fe_{0.008}Sb_{1-x}Se_x$ thin films thermally evaporated on Silicon substrate having resistance of the order of Ohm to Kilo Ohm at RT which is discussed in chapter 4.

2.5.1.3 Quantum Design Physical Property Measurement System

Quantum Design Physical Property Measurement System (PPMS) is used for Resistivity measurements at low temperature down to 2 K and high magnetic fields up to 14 T shown in **figure 2.12**. The photograph of cross section of QD PPMS diagram which shows inner parts of it shown in **figure 2.13**.
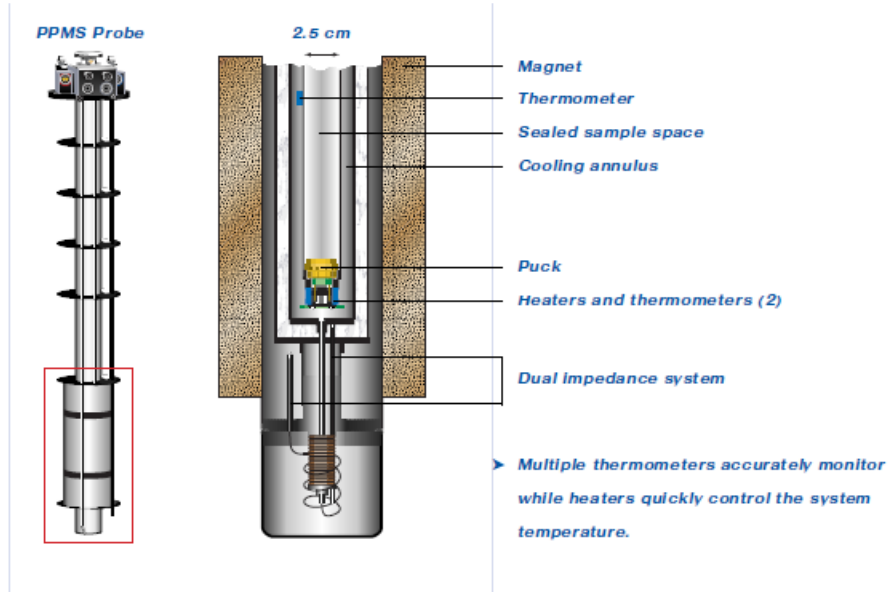
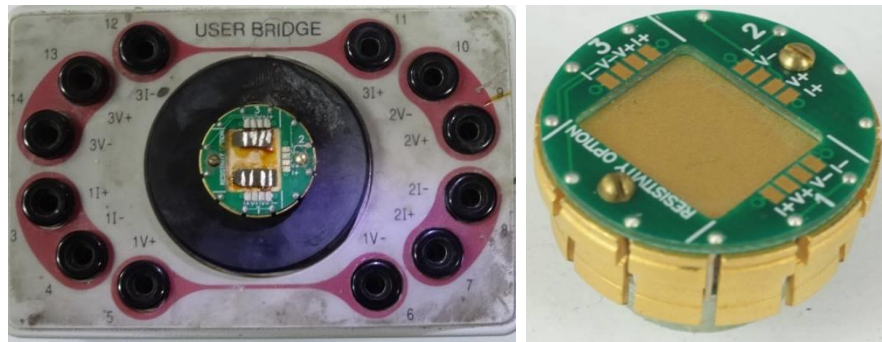*Figure 2.12: Physical property measurement System*

Liquid nitrogen reservoir

High-T$_c$ Magnet Leads

Liquid helium reservoir

PPMS probe inserted through top of dewar

Magnet protection circuit

Oxford Instruments 16 tesla magnet mounted inside dewar

Figure 2.13: Internal structure of PPMS Dewar

It shows liquid Helium (LHe^4) reservoir surrounded by liquid Nitrogen (LN$_2$) reservoir. A 14 T magnet is mounted in LHe^4 reservoir as shown. **Figure 2.14** shows PPMS probe with a baffle and connections of parts. The red highlighted portion of the left one is shown in right side with the zoomed one.

42

Figure 2.14: Cross sectional view of PPMS with RT pucks

Figure 2.15: Puck holder left and puck at right in PPMS system

Cooling annulus is outside of the chamber. The puck is placed inside a sample chamber in the region of uniform magnetic field. Platinum resistance thermometer (PRT) is arranged on the chamber wall. Bottom of the puck, heater and cernox thermometer are arranged. **Figure 2.15** shows the puck holder in the PPMS system (left side) and puck (right side). The PPMS system is used for the electrical (R-T) as well as resistance as a function of magnetic field (R-H) studies of transition metal (Fe, Co, Ni and Mn) doped InSb thin films, which is thermally evaporated on Silicon substrate discussed in chapter 5.

2.6 Hall Effect Measurement

The Hall Effect is a conducting phenomenon of a material, involving moving charge particles in conductors under the influence of the Lorentz force. If an electric current flows through a conductor in a magnetic field, the magnetic field exerts a transverse Lorentz force which tends to push them to one side of the conductor. A buildup of charge on the sides of the conductors will balance this magnetic influence, producing a measurable transverse voltage between the two opposite sides of the conductor. The presence of this measurable transverse voltage is called the Hall voltage and the phenomenon is called Hall Effect.

2.6.1 Ordinary Hall Effect

The ordinary Hall Effect provides a relatively simple method for determining accurately carrier density, electrical resistivity and the mobility of carriers in semiconductors due to its simplicity, low cost and fast turnaround time. Thus, the ordinary Hall measurement is regarded as an essential characterization technique for the semiconductor industry and in research laboratories.

2.6.2 Anomalous Hall Effect

In ferromagnetic materials (and paramagnetic materials in a magnetic field), the Hall resistivity includes an additional contribution, known as the anomalous Hall Effect (also known as an extraordinary Hall Effect or spontaneous Hall Effect), which depends directly on the magnetization of the material, and is often much larger than the ordinary Hall Effect. The anomalous Hall coefficient can be expressed in the following form [27].

$$\rho_{Hall} = R_0 B + R_s M$$

Where $R_0 B$ is the term due to the ordinary Hall Effect, M is magnetization of the sample under test. By finding the anomalous Hall coefficients, the magnetization can be

determined. Therefore, the anomalous Hall Effect is recognized as a useful tool for measuring the magnetic hysteresis M(H) loops of DMSs. Although a well-recognized phenomenon, there still debate about its origin in various materials. The anomalous Hall Effect can be either an extrinsic (disorder-related) effect due to spin-dependent scattering of the charge carriers or an intrinsic effect which can be described in terms of spin chirality or the Berry phase effect in the crystal momentum space.

The electrical resistivity of a semiconductor thin film can be written using Ohm's law,

$$\rho = \frac{1}{en\mu}$$

Where 'ρ' is the film resistivity, 'e' is the electronic charge, n is the number of carriers corresponding to the carrier concentration and 'μ' is the carrier mobility. According to Ohm's law the carrier mobility affects resistivity. Low resistivity can be achieved by increasing the carrier concentration or mobility or both. Increasing carrier concentration is self-limiting because at some point the increased number of free carriers decreases the mobility of the film due to carrier scattering. Hence there is a trade-off between the carrier density and carrier mobility for achieving low resistivity.

In the case of Iron doped $Sb_{1-x}Se_x$ alloy thin films, the resistivity (ρ), carrier concentration (n), carrier mobility (μ), and sheet resistance are measured using Van der Pauw four-point probe in geometry. Samples used are 1 cm $\times$ 1 cm in size. The Ohmic contacts are made using a silver paste. The silver paste is applied at the corners of the sample symmetrically.
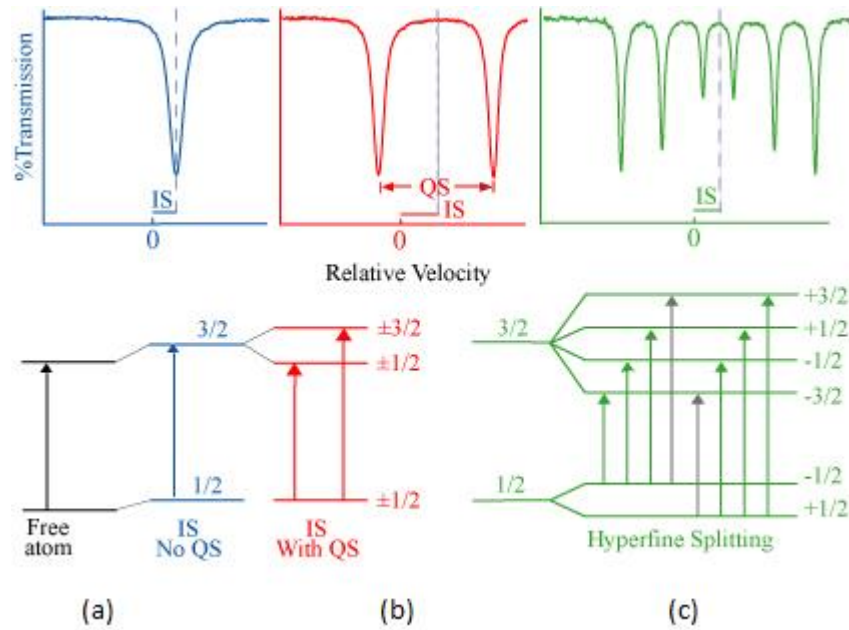
Figure 2.16: *Ecopia HMS-3000 Hall Measurement System*

The Hall measurement is performed using *Ecopia HMS 3000 Hall measurement system* with magnetic field of 0.55 tesla at IUAC, New Delhi, India (laboratory photograph is shown in **figure 2.16**) on the $Fe_{0.008}Sb_{1-x}Se_x$ thin films grown on Silicon substrate with a thickness of 500 nm. The details are discussed in chapter 4.

2.7 Mossbauer Spectroscopy

Mossbauer spectroscopy is a very sensitive tool to study hyperfine interactions. It can provide precise information about the chemical, structural, magnetic and time dependent properties of a material. The phenomenon of recoil-free emission and absorption of gamma rays from nuclear transitions without loss of energy is known as Mossbauer Effect [28-30], named after its discoverer Rudolf Mossbauer, a graduate student at the Max-Planck Institute in Heidelberg, observed this effect in 1957 and received the Nobel Prize in 1961. The Mossbauer Effect provides information about the local magnetic and electronic environment surrounding the Mossbauer nuclei such as ^{57}Fe or ^{119}Sn in a sample. This technique does not require any kind of external field and it is possible to observe very weak magnetic interactions without perturbing the effect of external fields [31-32]. The essence of the Mossbauer Effect is the absorption of

recoil momentum by the entire lattice of the solid. Since the lattice is much more massive than the nucleus, its recoil kinetic energy is effectively zero. In this case the gamma rays carry away the energy.

Figure 2.17: *Hyperfine interaction scheme for the ^{57}Fe Mossbauer transition induced by Coulomb interaction (isomer shift), quadrupole interaction and magnetic interaction between the nucleus and the electrons*

Thereby the emission and absorption lines overlap. In the experiment a source containing ^{57}Co nuclei provides a convenient supply of excited ^{57}Fe nuclei, which decay into the ground state accompanied by a gamma ray emission (**figure 2.17**). When the gamma ray energy matches resonantly with the energy level of absorbing nuclei, then transition occurs through absorption. For this purpose, the source moves with a certain velocity v and the frequency of gamma photon, the Doppler shifts can be quite significant. In this way one can probe any splitting in the ground state in the source or absorber nucleus which might result from magnetic or other interactions. **Figure 2.17** shows the absorption peak occurring at v = 0, since source and absorber are identical. The energy levels in the absorbing nuclei may be in three different environment, *i.e*

isomer shift (**figure 2.17a**), quadrupole splitting (**figure 2.17b**) and magnetic splitting (**figure 2.17c**).

2.7.1 Isomer shift

The isomer shift arises due to a slight change in the coulomb interaction between the nuclear and electronic charge distributions over the nuclear volume, which is associated with a slight increase of the ^{57}Fe nucleus in the I = 3/2 state. As the isomer shift is proportional to s electron density of the nucleus, this can be used to gain information about the valence state of the Mossbauer atom or of charge transfer. Also, it is useful to detect lattice expansion or compression, as these also changes the electron density **[33].**

2.7.2 Quadrupole splitting

If the nucleus is subjected to an electric field gradient, the interaction between the nuclear quadrupole moment and the electric field gradient splits the excited state I = 3/2 into a doublet (a two-line spectrum produced) and this splitting is called quadrupole splitting **[34].** Its applications are the investigation of local symmetry around the Mossbauer atom and the configuration of its valence electron.

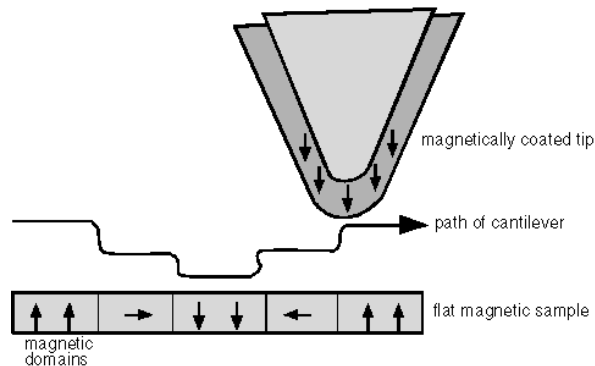## 2.7.3 Magnetic splitting (Zeeman splitting)

In the presence of a magnetic field, the nuclear spin moment experience a dipolar interaction with the magnetic field *i.e.* Zeeman splitting. There are many sources of magnetic fields that can be experienced by the nucleus. The total effective magnetic field of the Mossbauer nucleus is given by $B_{eff} = B_{contact} + B_{orbital} + B_{dipolar} + B_{applied}$ **[35-40].** The first three terms being due to the atoms own partially filled electron shells. $B_{contact}$ is due to the spin on those electrons polarizing the spin density at the nucleus, $B_{orbital}$ is due to the orbital moment on those electrons and $B_{dipolar}$ is the dipolar field due

to the spin of those electrons. This effect can be used to detect magnetic exchange interactions and local magnetic fields [41].

The Mossbauer spectroscopy is used to observe the hyperfine interaction of Iron doped transition metal doped InSb bulk system discussed in chapter 5.

2.8 Magnetic force Microscopy (MFM)

Magnetic Force Microscopy (MFM) is one of the most important tools for studying the magnetic structure of ferromagnetic and magnetic semiconductor thin films. MFM has been developed from the earlier form of microscopy, in which the alternating voltage on the probe tip is replaced with an alternating field. This technique is based on the forces between a very small ferromagnetic tip attached to a flexible cantilever and the inhomogeneous stray field immediately outside a specimen of interest.

Figure 2.18: MFM maps the magnetic domains of the sample surface

The tip is used to probe the magnetic stray field above the specimen surface. The magnet tip is mounted on a small cantilever which translates the force into a deflection that can be measured as shown in **figure 2.18**. The microscope can sense the deflection of the cantilever, which will result in a force image (static mode) or the resonance frequency change of the cantilever, which will result in a force gradient image. The sample is scanned under the tip, which results in a mapping of the magnetic force or

force gradients above the surface.

One of the most crucial part of the image formation process in an MFM technique is the force sensor by a tiny magnetic tip mounted on a flexible beam (cantilever) artifacts due to the usually unknown magnetic state of the tip, its influence on the sample magnetization may lead to image perturbations and misinterpretations. To get quantitative information out of MFM measurement tips with well- defined magnetic status are required.

To analyze domain pattern in thin films of the selected system MFM has been carried out on a NANOSCOPE III a (digital instruments) at UGC DAE CSR, Indore (M.P.).

The MFM is used to observe the magnetic interaction of the $Fe_{0.01}Ge_{1-x}Sb_x$ (chapter 3), $Fe_{0.008}Sb_{1-x}Se_x$ (chapter 4) and transition metal doped InSb thin films (chapter 5) respectively.

2.9 Optical Studies

Experimental technique such as photoluminescence is used in order to perform the optical studies of the prepared thin films and nanostructures. A brief note on photoluminescence study is given below.

2.9.1 Photoluminescence (PL)

Optical transitions provide direct access to the energy level band development structure of a system. Photons of a particular energy that are absorbed or emitted by a sample provide evidence of electronic states differing by that energy within the material. Absorption is a good probe of the overall band structure of a system because bands have a relatively high density of states. PL emission, on the other hand, tends to favor sparse low-lying states because photo excited carriers rapidly thermalize through bands and closely spaced states to within kT of the lowest available levels. This feature

of PL makes it particularly effective in the analysis of interfaces where discrete defect and impurity states abound. If the state is radiative, it will generate unique peaks in the PL spectrum **[42-44]**.

The PL spectra is used for the studies of $Fe_{0.008}Sb_{1-x}Se_x$ films (chapter 4).

References

[1]. L. I. Maissel and R. Glang, *Hand Book of Thin film Technolog*, Mc.Graw Hill, New York (1970).

[2]. W. Gaede, *Ann Physik*, **46** 357 (1915).

[3]. K. L. Chopra and K. L. Malhotra, *Thin film technology and Applications*, Mc Graw Hill, New york (1985).

[4]. W. A. Bryant *J. Mater. Sci.*, **12(7)** 1285 (1977).

[5]. R. N. Ghoshtagore *J. Electrochem. Soc.* **125(1)** 110 (1978).

[6]. T. Suntola *Thin Solid Films* **216(1)** 84 (1992).

[7]. R. R. Chamberlin and J.S. Skarman *J. Electrochem. Soc.* **113(1)** 86 (1966).

[8]. C. J. Brinker, A. J. Hurd, G. C. Frye, K. J. Ward and C.S. Ashley *J. Non- Cryst. Solids* **121** 294 (1990).

[9]. C.C. Chen, M.M. Nasrallah, and H. U. Anderson *J. Electrochem. Soc.* **140 (12)** 3555 (1993).

[10]. C. J. Brinker, G. C. Frye, A. J. Hurd, and C. S. Ashley *Thin solid Films* **201(1)** 97 (1991).

[11]. K. M. K. Srivatsava, Deepak Chhikara and M. Senthil Kumar *J. Mater. Sci. Technol.* **27(8)** 701 (2011).

[12]. D. S. Chuu, C. M. Dai, W. F. Hsieh and C. T. Tsai *J. Appl. Phys.* **69** 8402 (1991).

[13]. V. R. Katti, A.K. Debnath, K.P. Muthe, Manmeet Kaur, A. K. Dua, S. C. Gadkari, S. K. Gupta, V. C. Sahni *Sensors and Actuators B* **96** 245 (2003).

[14]. N. Tigau, V. Ciupina, G. Prodan, G. I. Rusu, E. Vasile *Journal of Crystal Growth* **269** 392 (2004).

[15]. S Velumani, J. A. Ascencio *Appl. Phys. A* **79** 153 (2004).

[16]. R. Indirajith, T. P. Srinivasan, K. Ramamurthi, R. Gopalakrishnan *Current Applied Physics* **10** 1402 (2010).

[17]. Milton Ohring, 'Material Science of Thin Films, deposition and structure', 2nd edition, Acadamic press San diego, California, USA-92101-4495 (1990).

[18]. D. L. Smith, *Thin films Deposition*. McGraw-Hill, New York (1995).

[19]. L. Holland, Vacuum Deposition of Thin Films, Wiley, New York (1956).

[20]. P. Scherrer, Gottinger Nachrichten, **2** 98 (1918).

[21]. C Richard Brundle, Charles A. Evans, Jr. and Shaun Wilson, *Encyclope- dia of Materials Characterization- Surfaces, Interfaces, Thin Films* (Massachusetts: Butterworch-Heinemann) **71** 99 203 (1992).

[22]. Ian M Watt, The Principles and Practice of Electron Microscopy *Cambridge: Cambridge University Press* **89** 413 (1997).

[23]. D. K. Schroder, Semiconductor material and device characterization. *New York John Wiley & Sons*, second Ed. (1998).

[24]. L. J. van der Pauw, "A method of measuring specific resistivity and hall effect of discs of arbitrary shape" *Philips Res. Rep.* **13** 1 (1958).

[25]. L. J. van der Pauw, "A method of measuring the resistivity and hall coefficient on lamellae of arbitrary shape", *Philips Technical Rev.*, 20(8), 220 (1958-1959).

[26]. S. H. Panwar, P. N. Bhosale *Mater. Chem. Phys.* **11** 461 (1984).

[27]. The Hall Effect and its applications, edited by C. L. Chien and C. R. Westgate Plenum, New York (1980).

[28]. R. L. Mossbauer *Z. Physik* **151** 124 (1958).

[29]. R. L. Mossbauer, Naturwissenssen schaften **45** 538 (1958).

[30]. R. L. Mossbauer Z Naturforsch **14a** 211 (1958).

[31]. Sauer Ch. and Zinn W. Magnetic multilayers eds. Bennet L. H. and Watson R. E.,

Singapore, World scientific (1993).

[32]. Wegener H. Der Mossbauer effect and seine Anwendung in Physik and Chemie Germany, Bibliograph Institut Mannheim (1966).

[33]. M. H. Cohen and F. Reif *Solid state physics* **5** 321 (1957).

[34]. W. Marshall and C. E. Johnson *J. Phys. Radium* **23** 733 (1962).

[35]. F. V. D. Wounde and G. A. Sawatzky *Phys. Rev. B* **4** 3159 (1971).

[36]. F. V. Wounde, Mossbauer spectroscopy and magnetic properties of iron compounds, *Ph.D. Thesis*, Netherlands, Groningen University, (1966).

[37]. F. V. D. Wounde *Phys. Stat. Solidi* **17** 417 (1966).

[38]. G. J. Perlow, C. E. Johnson and W. Marshall *Phys. Rev.* **140A** 875 (1965).

[39]. E. J. Sharp and J. E. Miller *J. Appl. Phys.* **41** 4718 (1970).

[40]. E. J. Sharp and J. E. Miller *J. Appl. Phys.* **40** 4680 (1969).

[41]. Sangeeta Thakur, Structural and Magnetic properties of Indium substituted Nickel-Zinc Ferrites Synthesized via Reverse Micelle Technique, Ph.D. Thesis, Jaypee University of Information Technology, Waknaghat, Himachal Pradesh, India (2010).

[42]. H. T. Grahn, "*Introduction to semiconductor physics*" World Scientific Publishing Co. Pte. Ltd, Singapore, 1999.

[43]. Bernard Valeur, *Molecular Fluorescence Principles and Applications*, Wiley, (2002).

[44]. Timothy H. Gfroerer, '*Photoluminescence in Analysis of Surfaces and Interfaces', Encyclopedia of Analytical Chemistry,* R.A. Meyers (Ed.) pp. 9209–923, Wiley (2000).